AADE-05-NTCE-27

Comparing a Basic Set of Drilling Fluid Pressure-Loss Relationships to Flow-Loop and Field Data

Mario Zamora, Sanjit Roy, and Ken Slater, M-I SWACO

This paper was prepared for presentation at the AADE 2005 National Technical Conference and Exhibition, held at the Wyndam Greenspoint in Houston, Texas, April 5-7, 2005. This conference was sponsored by the Houston Chapter of the American Association of Drilling Engineers. The information presented in this paper does not reflect any position, claim or endorsement made or implied by the American Association of Drilling Engineers, their officers or members. Questions concerning the content of this paper should be directed to the individuals listed as author/s of this work.

Abstract

This paper is an extension of a recent AADE publication that introduced the Unified model as a practical rheological characterization of Herschel-Bulkley fluids. Equations have been added to handle other important hydraulics issues, including pressure losses in transitional and turbulent flow. By intent, most of the relationships are already in use by at least part of the drilling industry, and are all direct and simple enough to use in a spreadsheet without complicated macros. A primary purpose of this paper is to compare results from this basic set of equations to laboratory and field measurements.

Pressure-loss data presented in this paper have been taken from various scale-up pipe and annular flow loops, full-scale yard tests, and an instrumented offshore well. The data encompass laminar, transitional, and turbulent flow regimes in pipe and annular flow (some with eccentricity). Fluid types include synthetic-based fluids and different compositions of water-based fluids.

For the most part, the data fit is good enough to suggest that the basic set of relationships is suitable for use in most industry hydraulics programs. Understandably, some fits are better than others, and some issues related to this critical topic still have not been resolved. Comments on these technology gaps and recommendations for further development also are included in this paper.

Introduction

A case was made in a recent paper[1] for the industry to develop a unified, basic set of equations to address drilling fluids hydraulics and rheology during drilling operations. The primary objective was to prevent high-end hydraulics software applications from becoming proverbial "black boxes" from the perspective of field engineers charged with applying this important technology. For this to succeed, the relationships would have to be as practical as possible, closely match current industry practices, and apply to critical and conventional wells alike.

An empirically derived flow equation based on the Herschel-Bulkley model was introduced to support this effort. Expressed in a form easily recognized by field engineers, the so-called Unified model was shown to be sufficiently accurate for most advanced hydraulics programs. The Herschel-Bulkley model had re-emerged as the model of choice for a many drilling fluids applications, primarily because it:

- fits a wide range of drilling muds,
- contains a yield-stress term that often is used to evaluate and optimize hole cleaning, barite sag, suspension, and other key hydraulics-related concerns, and
- includes as special cases the traditional Bingham plastic model and exact power law depending on the value of yield stress.

In this paper, additional equations are presented to calculate pipe and annular frictional pressure losses in laminar, transitional, and turbulent flow. They are applicable to water, oil and synthetic-based fluids, but do not address air/gas, foam, and other aerated or highly compressible fluids. The relationships follow the same practical constraints applied to the Unified model development. Most already are in use by at least part of the drilling industry; all are direct and simple enough to use in a spreadsheet without needing complicated macros or goal-seek techniques. A method for calculating critical velocity is included in the Appendix.

A primary focus of this paper is to compare results from this basic set of equations to pressure-loss measurements taken in laboratory flow loops and larger-scale yard tests. "Scale-up" flow loops, built from small-diameter conduits to limit laboratory space and fluid volumes, are used to predict frictional pressure losses for the same fluid in large-diameter conduits. "Yard" tests use longer, larger-diameter conduits, sometimes using reeled coiled tubing.

Data considered in this paper were taken from five different sources under a range of conditions, including pipes and annuli (some with eccentricity). Fluid types include synthetic-based fluids and various compositions of water-based fluids. Simulations also are compared to data taken on an instrumented well in the Gulf of Mexico, although the density and temperature profiles that exist in actual wells are beyond the scope of this paper.

Frictional Pressure-Loss Equations

Equations presented here are essentially the column variables required to construct a pressure-loss spreadsheet with flow rate Q as the independent variable. For flow-loop experiments, the sequence of rows would start with flow rate; test-section geometry and mud properties do not change. For calculating pressure losses in a well, the rows would be constructed around depth intervals (or section lengths); each

row would have its own set of well geometry and mud properties, but a single flow rate would apply to all rows. Drillstring and annular pressures would be the summation of the calculated pressures in each row for different flow-rate values. Both approaches would produce a matched array of pressures and flow rates.

Geometric Parameters L, d_h, d_p, d_i, d_{hyd}, and e. Flow-loop and sectional geometry include the length L, hole diameter d_h, and external and internal pipe diameters d_p and d_i, respectively. The most widely used expression for annular hydraulic diameter is $d_h - d_p$, which is based on the ratio of the cross-sectional area to the wetted perimeter; for pipes, it is the internal diameter d_i. Annular configurations should include an eccentricity parameter e, where $e = 0$ for a concentric annulus and $e = 1$ for a fully eccentric annulus.

Flow loops are considered to have a singular geometry, although some are configured with serial and parallel test sections of different diameters. In a well, a geometric section is defined for every change in casing or pipe diameters. For deepwater, HTHP and highly deviated wells, the drillstring and annulus should further subdivided into short (50 to 100-ft) segments in order to allow for effects of temperature and pressure on density and rheological properties.

Fluid Properties ρ, PV, YP, τ_y, n, and k. Mud density and rheological properties should be maintained constant during flow-loop testing. This means that fluid temperature should not vary appreciably during the entire test procedure. For critical wells, density and rheological parameters should be defined in each well segment.

Rheological properties used for pressure-loss calculations are measured on field and HTHP laboratory viscometers. The traditional oilfield parameters are plastic viscosity PV, yield point YP, and yield stress τ_y. The low-shear yield point ($LSYP = 2R_3 - R_6$) is often used to approximate true yield stress. Herschel-Bulkley model parameters n, k, and τ_y are derived from these oilfield rheological measurements using the following equations:

$$n = 3.32\log_{10}\left(\frac{2PV + YP - \tau_y}{PV + YP - \tau_y}\right) \quad \text{... (1)}$$

$$k = \frac{PV + YP - \tau_y}{511^n} \quad \text{... (2)}$$

Some complex relationships for Herschel-Bulkley fluids are difficult and even impossible to evaluate analytically. At high shear rates, it is acceptable to treat Herschel-Bulkley fluids as power-law fluids in order to take advantage of existing relationships. The assumption is that the log-log slope of the Herschel-Bulkley flow equation is numerically close to the power-law flow behavior index n_p.

$$n_p = 3.32\log_{10}\left(\frac{2PV + YP}{PV + YP}\right) \quad \text{... (3)}$$

Velocity V. The mean velocity V is directly proportional to flow rate and inversely proportional to the cross-sectional area of the fluid conduit.

$$V = \frac{24.51Q}{d_i^2} \quad \text{(Pipe)} \quad \text{... (4a)}$$

$$V = \frac{24.51Q}{d_h^2 - d_p^2} \quad \text{(Annulus)} \quad \text{... (4b)}$$

Shear Rate at the Wall γ_w. Shear rate at the wall γ_w, required to calculate the shear stress at the wall, is the product of the Newtonian shear rate and a geometry factor G. The result applies to pipes and annuli for appropriate values of fluid velocity V and hydraulic diameter d_{hyd}.

$$\gamma_w = \frac{1.6GV}{d_{hyd}} \quad \text{... (5)}$$

The correction factor given in Eq. 6 adjusts for flow conduit geometry. An additional correction for oilfield viscometers is not included here because a closed analytical solution for Herschel-Bulkley fluids does not exist and the impact is not considered overly significant. Factor G is dependent on the rheological parameter n and a geometry factor $\alpha = 0$ for pipes and $=1$ for annuli (assuming parallel-plate flow).[2]

$$G = \left[\frac{(3-\alpha)n + 1}{(4-\alpha)n}\right]\left[1 + \frac{\alpha}{2}\right] \quad \text{... (6)}$$

Shear Stress at the Wall τ_w. Frictional pressure loss is an increasing function of the shear stress at the wall τ_w defined by the fluid-model-dependent flow equation. Flow equations for Bingham plastic and Herschel-Bulkley fluids are complex and their exact solutions are usually found by iterative means. However, they can be approximated by the Unified model flow equation that is of the same recognizable form as the respective constitutive equations:[1]

$$\tau_w = 1.066\left[\left(\frac{4-\alpha}{3-\alpha}\right)^n \tau_y + k\gamma_w^n\right] \quad \text{... (7)}$$

For $\tau_y = 0$, Eq. 7 reduces to the exact solution for power-law fluids. For $\tau_y = YP$, then $n = 1$ and Eq. 7 reduces to the simplified Bingham-plastic expression widely used in drilling. The constant 1.066 converts units from viscometer dial reading to $lb_f/100\ ft^2$.

Generalized Reynolds Number N_{ReG}. The generalized Reynolds number N_{ReG} is used to define the flow regime and to determine the friction factor. The most convenient form of the equation involves the shear stress at the wall τ_w.

$$N_{\mathrm{Re}G} = \frac{\rho V^2}{19.36\tau_w} \quad \text{... (8)}$$

Friction Factor Laminar Flow f_{lam}. Laminar-flow friction factors f_{lam} for pipes and concentric annuli are combined into a single relationship when using the generalized Reynolds number N_{ReG} defined in Eq. 8.

$$f_{lam} = \frac{16}{N_{\mathrm{Re}\,G}} \quad \text{... (9)}$$

Friction Factor Transitional Flow f_{trans}. An empirical equation consistent with the Churchill[3] method presented later and the commonly accepted expression for critical Reynolds number[4] can be used to approximate the transitional-flow friction factor f_{trans}:

$$f_{trans} = \frac{16 N_{\mathrm{Re}G}}{(3470 - 1370n)^2} \quad \text{... (10)}$$

Friction Factor Turbulent Flow f_{turb}. The Blasius form of the turbulent-flow friction factor f_{turb} for non-Newtonian fluids is a function of generalized Reynolds number N_{ReG} and the rheological parameter n_p. The expressions for a and b are based on curve fits of data taken on power-law fluids.[4]

$$f_{turb} = \frac{a}{N_{\mathrm{Re}G}^{b}} \quad \text{... (11)}$$

where,

$$a = \frac{\log_{10}(n_p) + 3.93}{50} \quad \text{... (12a)}$$

$$b = \frac{1.75 - \log_{10}(n_p)}{7} \quad \text{... (12b)}$$

Fanning Friction Factor f. Pressure losses in pipes and annuli are proportional to the Fanning friction factor f which in turn is a function of generalized Reynolds number, flow regime, and fluid rheological properties. The Churchill[3] method can be used to determine the friction factor f for any Reynolds number and flow regime. This technique involves an intermediate term f_{int} based on transitional and turbulent-flow friction factors f_{trans} and f_{turb}, respectively, and the laminar-flow friction factor f_{lam}.

$$f = \left(f_{\mathrm{int}}^{12} + f_{lam}^{12}\right)^{1/12} \quad \text{... (13)}$$

where,

$$f_{\mathrm{int}} = \left(f_{trans}^{-8} + f_{turb}^{-8}\right)^{-1/8} \quad \text{... (14)}$$

Frictional Pressure Loss P. The Fanning equation is the basic relationship for calculating frictional pressure loss P in pipes and annuli. The defining parameter is the Fanning friction factor f, which depends on the generalized Reynolds number, flow regime, and fluid rheological properties. The other four parameters (density ρ, velocity V, length L, and hydraulic diameter d_{hyd}) are measured or easily calculated directly in flow-loop tests, as long as the fluid temperature does not change appreciably in the main test section. Eq. 15 also can be used to calculate pressure losses in actual wells if allowances are made for geometrical changes and the effects of temperature and pressure on downhole rheological properties and density.[5]

$$P = \frac{1.076 \rho V^2 f L}{10^5 d_{hyd}} \quad \text{... (15)}$$

Eccentricity Correction R_{lam} and R_{turb}. Drillstring eccentricity e in directional wells reduces annular pressure loss in laminar and turbulent flow. A widely used method[6] to estimate the magnitude of this reduction is based on the product of the concentric-annulus pressure loss and the empirically derived ratio R_{lam} or R_{turb} depending on the flow regime. The value of e is 0 for concentric annuli and 1 for fully eccentric annuli (only absolute values for e should be used regardless of positive or negative eccentricity).

$$R_{lam} = 1.0 - 0.072\frac{e}{n}\left(\frac{d_p}{d_h}\right)^{0.8454} - \frac{3}{2}e^2\sqrt{n}\left(\frac{d_p}{d_h}\right)^{0.1852} + 0.96e^3\sqrt{n}\left(\frac{d_p}{d_h}\right)^{0.2527} \quad \text{... (16a)}$$

$$R_{turb} = 1.0 - 0.048\frac{e}{n}\left(\frac{d_p}{d_h}\right)^{0.8454} - \frac{2}{3}e^2\sqrt{n}\left(\frac{d_p}{d_h}\right)^{0.1852} + 0.285e^3\sqrt{n}\left(\frac{d_p}{d_h}\right)^{0.2527} \quad \text{... (16b)}$$

Special Considerations. There are various pressure-related issues observed in the field and in laboratory testing that have not been resolved to the extent where practical relationships are available. These include the following:

- *Drillstring Rotation*. Pipe rotation invariably increases annular pressure loss in the field, especially in directional and slimhole wells. Unfortunately, relationships are not available that consider combined effects of rotation, non-Newtonian fluid behavior, eccentricity, and hydro-dynamic/drillstring instabilities.[7] Part of the pressure increase in directional wells may be attributed to cuttings or sagged weight material incorporated into the main flow stream. Most hydraulics studies on the subject have focused on slimhole geometry where narrow annular clearances can magnify the effects of rotation.[8]
- *Pipe Roughness.* Pipe roughness elevates the friction factor in fully developed turbulent flow; however, the relative roughness for most wellbore geometries is low, and the Reynolds numbers in pipes and annuli rarely reach the high values where the effects of roughness are most significant.[9]
- *Drag Reduction.* Low-solids, viscoelastic fluids in turbulent flow exhibit delayed onset of turbulence and lower friction factors and pressure losses. Various analytical and empirical techniques have been proposed to model this behavior, but none have been universally adapted for drilling fluids.[10]
- *Tool Joints*. Tool joints can increase pressure losses in the annulus[11] and in the drillstring due to geometry effects, and fluid contraction and expansion. Internally constricted tool joints can further increase drillstring losses because of the apparent inability of the fluid to recover from full turbulence (where $P \propto Q^2$) after entering the drill-pipe tube. This can dramatically increase the turbulent flow friction factor and pressures at high flow rates.[12] One method to account for this behavior is to empirically adjust the Blasius constants a and b from Eqs. 12a-12b.
- *Coiled Tubing.* Frictional pressure losses for coiled tubing on the reel are higher than for straight tubing due to imposed secondary flows.[13] A number of correlations

have been published to compensate for this effect by adjusting the friction factors in laminar and turbulent flow.[14] However, most of these modifications are empirically derived and are difficult to generalize due to their high sensitivity to drilling fluid characteristics.

Graphical Analysis Options

The simplest graph for analyzing measured data is a rectilinear plot of pressure versus flow rate. In this type of graph, curve segments that are concave upwards ("hold water") indicate turbulent flow; concave downwards segments reflect laminar flow. Limitations of this graphical method include difficulties (a) determining flow parameters, (b) identifying flow-regime transitions, and (c) directly comparing results from different geometries.

The log-log plot (rheogram) of wall shear stress τ_w versus Newtonian shear rate γ (defined by Eqs. 17 and 18, respectively) is a universal graphical method for analyzing measured data from flow loops.

$$\tau_w = \frac{300 P d_{hyd}}{L} \quad \text{... (17)}$$

$$\gamma = 1.6\left(1+\frac{\alpha}{2}\right)\frac{V}{d_{hyd}} \quad \text{... (18)}$$

In Eq. 17, pressure P is the measured pressure, regardless of flow regime. The three flow regimes are usually evident if the shear-rate range is sufficient. Flow parameters can be determined from the laminar portion of the flow curve, which is geometry independent. The transitional and turbulent regions, unfortunately, are not (departure from the laminar curve depends on conduit geometry). Viscometer data can be superimposed, but the Fann geometry precludes turbulent flow.

The modified Moody (friction-factor) chart provides a broader perspective in that laminar, transitional, and turbulent regimes are easily identified and compared regardless of geometry. The basic chart shown in **Fig. 1** is based entirely on Eq. 13 and its predecessors. Friction factors f, f_{lam}, f_{trans}, and f_{turb} are functions of N_{ReG} and n (or n_p). For this analysis, friction factor f from Eq. 13 can be plotted on logarithmic coordinates versus generalized Reynolds number N_{ReG} calculated by Eq. 8. Alternatively, Eq. 15 can be rearranged to determine friction factor f from measured pressure P, permitting comparison of modeled and measured friction factors.

Comparisons to Measured Data

Considerable data have been taken and analyzed over time by the drilling industry with the goal of developing suitable relationships for calculating pressure losses. Unfortunately, the raw data and/or critical testing details are rarely available for subsequent analyses by others for a number of very valid reasons. Some data are presented here from several sources to compare to the basic set of equations provided in this paper. Fluids used in these tests are summarized in **Table 1**. The rheological parameters were measured on multi-speed, rotational viscometers. The following are the different facilities used for testing:

- *Test Facility 1* - Amoco's Catoosa facility used for a master's thesis[15] study of pressure-loss correlations. The experimental facility consisted of two 5.023-in x 2.375-in. annular sections (concentric and fully eccentric), two 4.5-in. drill-pipe sections (with 3.826-in. and 3.640-in. IDs and one tool joint in each), and three 2.875-in. new and used tubing sections. Data files were obtained through the API. Tool joints are not considered in the calculations in this paper.
- *Test Facility 2* - scale-up flow loop originally constructed to evaluate slimhole hydraulics.[8] The 1.75-in. x 1.25-in. annular section (5.5 ft between differential pressure taps) was designed for variable eccentricity and shaft rotary speeds to 900 rpm. Rotation data are not present here.
- *Test Facility 3* - small-diameter, scale-up flow loop used primarily to study drag reduction. Multiple diameters were available, but data included in this paper are limited to those taken on 0.305-in. ID smooth tubes (5.5 ft between pressure taps).
- *Test Facility 4* - coiled-tubing unit at Alaska mud plant. A 28-ft long by 1.665-in. ID straight section was added to 15,600 ft, 2.375-in. OD x 1.995-in. ID coil tubing.
- *Test Facility 5* - coiled-tubing unit at Louisiana mud plant. A 2.41-in. ID straight tube (19.125 ft between differential pressure taps) was added to a 4,896-ft by 2.448-in. ID reeled coil tubing.
- *Test Facility 6* - instrumented offshore well.[12,16] The Gulf of Mexico well was being drilled in 420 ft of water, with 12,439 ft of 5-in. drill pipe inside of 12,710 ft of 11.875-in. casing. Downhole sensor packages were placed at three locations in the drillstring to measure internal and annular pressures and temperatures.

Fig. 2 is a pressure vs flow rate graph for a 26-lb/bbl bentonite slurry tested in the pipe and annular sections at Catoosa (Test Facility 1). Agreement among measured and calculated values is excellent for this example, except that the flow regimes are very difficult to delineate. The same data set was used to generate the Fanning friction-factor chart shown in **Fig. 3**. Results are still very good, plus the transitions from laminar to turbulent are now clearly evident.

Fig. 4 is a rheogram for a 33-lb/bbl bentonite slurry tested in the drill-pipe section at Test Facility 1. Fann viscometer data are superimposed to compare laminar flow behavior (the viscometer will not achieve turbulence). Results are very good. Typically, temperature and shear history are among the most common causes for incompatibility. This is illustrated in the friction-factor chart in **Fig. 5**. Pipe and annular values in laminar flow are well synchronized, but noticeably below model results based on viscometer data. Because the test fluid was a thermally sensitive ester-based fluid, it is highly likely that rheological measurements on the viscometer and flow-loop tests were run at different temperatures.

Turbulent flow is historically among the most difficult to model. This is especially true for water-based polymer fluids which can exhibit drag reduction, as demonstrated in **Fig. 6**. The low-solids, viscoelastic test fluid was formulated with 1.5 lb_m/gal of welan gum biopolymer. Turbulent flow was achieved in the drill pipe, but not in the annular section. For the pipe, the measured turbulent friction factor was significantly lower than expected. Additionally, the onset of turbulence was noticeably delayed.

Figs. 7 and **8** demonstrate the effects of eccentricity on annular pressure loss measured on Test Facility 2 using a lab-prepared and a field biopolymer fluid, respectively. The lab-prepared fluid was formulated with 2-lb/bbl xanthan gum. Solids lines in the graphs are based on pressure predictions adjusted for eccentricity using Eq. 16a. The excellent agreement among measured and calculated values helps validate the laminar-flow correction for eccentricity. Turbulence was not achieved in either example.

Friction-factor charts for two fluids tested in the small-diameter flow loop (Test Facility 3) are presented in **Figs. 9** and **10**. Comparisons between measured and calculated values are very good for these tests. The fluid in **Fig. 9** was a low-viscosity sample consisting of 20-lb/bbl unhydrated bentonite in a 5% NaCl brine. The 13.5-lb_m/gal fluid summarized in **Fig. 10** was weighted by ultra-fine, polymer-coated barite.

A similar fluid weighted by ultra-fine, polymer-coated barite was also tested in Test Facility 4, which consisted of a coiled-tubing unit and an attached short, straight pipe. Results are presented in **Fig. 11**. The short-pipe comparison is very good, but the measured data in the reeled coil was below the prediction in turbulent flow using one of the available correlations.

The data in **Fig. 12** was also generated using Test Facility 4, this time involving a special fluid containing hollow glass spheres. As in the previous example, an excellent match between measured and calculated data was obtained for the pipe section. The comparison for the reeled coiled tubing was more acceptable. This is evident in the **Fig. 13** friction-factor chart for the same data.

Fig. 14 is an interesting rheogram plot that contrasts testing of the same 14.2-lb_m/gal polyalpha olefin synthetic-based mud on three different geometries from Test Facilities 3 and 5. The first observation is that the coiled-tubing shear stress, as expected, is higher than in the straight pipe from Test Facility 5. Departures from laminar flow were at about 200 and 650 s^{-1} for the pipe and coil, respectively. Also, results from Test Facility 3 are superimposed to illustrate the geometry effect in transition and turbulent flow regimes when analyzing data using rheogram plots.

Figs. 15 and **16** are based on surface and downhole measurements made on an instrumented well[12,16] in the Gulf of Mexico (Test Facility 6) with a synthetic-based drilling fluid in the hole. **Fig. 15** compares measured and calculated annular pressures; **Fig. 16** provides comparisons for the drillstring. Pressure losses were calculated using equations presented in this paper after rough adjustments to consider temperature and pressure effects on downhole density and rheology in 1,000-ft segments. Corrections also were included for the slight drillstring eccentricity.

Measured annular pressure losses are plotted while ramping the flow rate up and down. Insufficient time was allotted for pressures to stabilize while ramping up, so these pressures are slightly over exaggerated. Otherwise the match between measured and calculated values is reasonable.

Attempts to match measured drillstring pressures were somewhat more difficult. The lower, dashed line in **Fig. 16** ignores calculations for the tool joints, which were highly constricted in this well.[12] Allowing for tool-joint geometry was helpful, but predictions were still lower than measured at high flow rates. Modifications to the turbulent flow friction factor relationships would be required to achieve additional improvements.

Epilogue

The great variety and complexities associated with drilling fluids and pressure-loss measurements can complicate rationalization of results. Process and procedure clearly are critical. However, even test results in smooth pipes run under controlled conditions in the laboratory will forever be difficult to translate into the field under downhole conditions.

Basic pressure-loss equations calculations presented in this paper fit measured data reasonably well in most cases. Major differences were encountered in turbulent flow, where all correlations have been empirically derived. Little data are available for Herschel-Bulkley fluids, but those historically used for power-law fluids seem adequate for the time being. Tool joints, especially those that are internally constricted, may require special attention. Also, it has not been possible to reliably model drag reduction in turbulent flow for water-based polymer fluids. In practice, the drag-reduction effect seen in clean fluids diminishes as drilled solids are incorporated.

In general, coiled-tubing data were difficult to match with available correlations. Problems probably were caused as much by the fluids tested as their behavior in the reeled tubing.

Spreadsheets used internally to test the simulations were not difficult to develop and manipulate. The well spreadsheet was somewhat more difficult because temperature and pressure effects on density and rheology were determined externally.

Finally, rheologists may be at odds with many, if not all, of the simplifications. On the other hand, field engineers might consider the list of equations and Greek symbols much too daunting. Every effort was made to simplify the process and the equations, without sacrificing content. Hopefully, others will find improved methods in the near future.

Conclusions

1. A basic set of equations has been presented to calculate frictional pressure losses for pipes and annuli.
2. The equations apply to laminar, transitional, and turbulent flow of Herschel-Bulkley fluids, with Bingham-plastic and power-law behavior as special cases.

3. Despite some complexities, the relationships are direct and simple enough to be programmed in spreadsheets without need for special macros.
4. Based on comparisons to results from scale-up flow loops, yard tests, and an offshore well, the data fit is good enough to suggest that the relationships are suitable for use in most industry hydraulics programs.
5. Understandably, some fits are better than others, and some aspects of this critical topic still have not been completely resolved, including drillstring rotation, pipe roughness, drag reduction, constricted tool joints, and coiled-tubing friction factors.
6. The basic set of equations can be used as the framework for further enhancements as additional flow-loop and well data are available.

Acknowledgements

The authors thank the management of M-I SWACO for supporting this work and for permission to publish. They also thank the University of Tulsa, the API, and all the individuals those who helped generate data presented in this paper.

References

1. Zamora, M. and Power, D.: "Making a Case for AADE Hydraulics and the Unified Rheological Model," paper AADE-02-DFWM-HO-13 presented at the Houston Chapter AADE Technology Conference, Houston, 2-3 April 2002.
2. Zamora, M. and Lord, D.L.: "Practical Analysis of Drilling Mud Flow in Pipes and Annuli," paper SPE 4976 presented at the 49th SPE Annual Fall Meeting, Houston, 6-9 Oct 1974.
3. Churchill, S.W.: "Friction Factor Equation Spans All Fluid-Flow Regimes," *Chemical Engineering* (7 Nov 1977) 91-92.
4. Schuh, F.J.: "Computer Makes Surge-pressure Calculations Useful," *Oil & Gas J* (3 Aug 1964) 96-104.
5. Zamora, M.: "Virtual Rheology and Hydraulics Improve Use of Oil and Synthetic-Based Muds," *Oil & Gas J* (3 Mar 1997) 43-55.
6. Haciislamoglu, M. and Cartalos, U.: "Practical Pressure Loss Predictions in Realistic Annular Geometries," paper SPE 28304 presented at the SPE Annual Technical Conference and Exhibition, New Orleans, 25-28 Sept 1994.
7. Hansen, S.A., *et al.*: "A New Hydraulics Model for Slim Hole Drilling Applications," paper SPE/IADC 57579 presented at the SPE/IADC Middle East Drilling Technology Conference, Abu Dhabi, 8-10 Nov 1999.
8. McCann, R.C., *et al.*: "Effects of High-Speed Rotation on Pressure Losses in Narrow Annuli," paper SPE 26343 presented at the SPE Annual Technical Conference and Exhibition, Houston, 3-6 Oct 1993.
9. Bourgoyne, A. T., *et al.*: *Applied Drilling Engineering*, SPE, Richardson, Texas (1991).
10. Govier, G.W. and Aziz, K.: *The Flow of Complex Mixtures in Pipes*, Robert E. Kreiger Publishing, Huntington, NY, (1977) 237-248.
11. Jeong, Y-T and Shah, S.N.: "Analysis of Tool Joint Effects for Accurate Friction Pressure Loss Calculations," paper IADC/SPE 87182 presented at the IADC/SPE Drilling Conference, Dallas, 2-4 Mar 2004.
12. White, W.W., Zamora, M. and Svoboda, C.F.: "Downhole Measurements of Synthetic-Based Drilling Fluid in Offshore Well Quantify Dynamic Pressure and Temperature Distributions," paper SPE 35057 presented at the SPE/IADC Annual Drilling Conference, New Orleans, 12-15 Mar 1996, and *SPE Drilling and Completion* (Sept 1997) 149.
13. Sas-Jaworsky II, A. and Reed, T.D.: "Predicting Pressure Losses in Coiled Tubing Operations," *World Oil* (Sept 1997) 141-146.
14. Zhou, Y. and Shah, S.N.: "New Friction Factor Correlations for Non-Newtonian Fluid Flow in Coiled Tubing," paper SPE 77960 presented at SPE Asia Pacific Oil and Gas Conference and Exhibition, Melbourne, 8-10 Oct 2002.
15. Subramanian, R.: "A Study of Pressure Loss Correlations of Drilling Fluids in Pipes and Annuli," Master of Science Thesis, The University of Tulsa (1995).
16. Svoboda, C. and Zamora, M.: "Collecting Detailed Downhole Hydraulics Data on an Offshore Rig: The Inside Story," presented at the Houston Chapter AADE Drilling Fluids Conference, Houston, 3-4 April 1996.

Nomenclature

a = Numerator in Blasius form of friction-factor equation
b = Exponent in Blasius form of friction-factor equation
B = Intermediate parameter used for critical velocity
d_h = Hole diameter or casing internal diameter, in.
d_{hyd} = Hydraulic diameter, in.
d_i = Pipe inside diameter, in.
d_p = Pipe outside diameter, in.
f = Fanning friction factor
f_{int} = Intermediate friction factor (transitional and turbulent)
f_{lam} = Friction factor (laminar)
f_{trans} = Friction factor (transitional)
f_{turb} = Friction factor (turbulent)
G = Geometry shear-rate correction (Herschel-Bulkley fluids)
G_p = Geometry shear-rate correction (power-law fluids)
k = Consistency factor (Herschel-Bulkley fluids), $lb_f s^n/100\ ft^2$
L = Length of flow loop, drill pipe or annular segment, ft
$LSYP$ = Low-shear yield point, °Fann ($\approx lb_f/100\ ft^2$)
n = Flow behavior index (Herschel-Bulkley fluids)
n_p = Flow behavior index (power-law fluids)
N_{ReG} = Generalized Reynolds number
P = Frictional pressure loss, psi
PV = Plastic viscosity, cP
Q = Flow rate, gal/min
R_3= Fann dial reading at 3 rpm, °Fann ($\approx lb_f/100\ ft^2$)
R_6= Fann dial reading at 6 rpm, °Fann ($\approx lb_f/100\ ft^2$)
R_{lam}= Pressure ratio for eccentric annulus (laminar)
R_{turb}= Pressure ratio for eccentric annulus (turbulent)
V = Velocity, ft/min
V_c = Critical velocity, ft/min
V_{cb} = Critical velocity Bingham-plastic fluids, ft/min
V_{cp} = Critical velocity power-law fluids, ft/min
YP = Yield point, °Fann ($\approx lb_f/100\ ft^2$)
α = Geometry factor (=0 for pipe and =1 for slot flow)
γ = Newtonian (nominal) shear rate, s^{-1}
γ_w = Shear rate at the wall, s^{-1}
ρ = Drilling fluid density, lb_m/gal
τ_w = Shear stress at the wall, $lb_f/100\ ft^2$
τ_y = Yield stress, $lb_f/100\ ft^2$

Appendix – Critical Velocity

While not required to calculate pressure losses, critical velocity is still an important hydraulics parameter. The critical velocity V_c is the bulk velocity where the Reynolds number N_{ReG} equals the critical Reynolds number (= 3470–1370n). The relationship for critical velocity is derived by substituting Eq. 5 into Eq. 7 and then the result into Eq. 8. Unfortunately, iterative or spreadsheet goal-seek methods are required to calculate V_c for Herschel-Bulkley fluids using Eq. A$_1$:

$$1.066\left[\left(\frac{4-\alpha}{3-\alpha}\right)^n \tau_y + k\left(\frac{1.6GV_c}{d_{hyd}}\right)^n\right] = \frac{\rho V_c^2}{19.36(3470-1370n)} \quad \text{... (A}_1\text{)}$$

A close approximation can be achieved by an empirical relationship based on the critical velocity for power-law fluids V_{cp}, critical velocity for Bingham-plastic fluids V_{cb}, and the τ_y/YP ratio. For power-law fluids, $\tau_y = 0$ and V_{cp} is calculated directly by:

$$V_{cp} = \left[\frac{28274(2.533-n_p)k_p}{\rho}\left(\frac{1.6G_p}{d_{hyd}}\right)^{n_p}\right]^{\frac{1}{2-n_p}} \quad \text{... (A}_2\text{)}$$

where,

$$G_p = \left[\frac{(3-\alpha)n_p+1}{(4-\alpha)n_p}\right]\left[1+\frac{\alpha}{2}\right] \quad \text{... (A}_3\text{)}$$

For Bingham plastics, $\tau_y = YP$ and $n = 1$, so V_{cb} can be calculated directly by the quadratic formula:

$$V_{cb} = \frac{67.86}{\rho}\left[B + \sqrt{B^2 + 9.42\rho YP\left(\frac{4-\alpha}{3-\alpha}\right)}\right] \quad \text{... (A}_4\text{)}$$

where,

$$B = \frac{PV\left(1+\frac{\alpha}{2}\right)}{d_{hyd}} \quad \text{... (A}_5\text{)}$$

Finally, the critical velocity V_c for Herschel-Bulkley fluids can be approximated by:

$$V_c = V_{cp} + (V_{cb} - V_{cp})\left(\frac{\tau_y}{YP}\right)^{\sqrt{\frac{V_{cp}}{V_{cb}}}} \quad \text{... (A}_6\text{)}$$

Table 1 - Fluids used for flow-loop and well testing

Test Facility	Fluid Type	ρ	PV	YP	τ_y	R
		lb_m/gal	cP	$lb_f/100\ ft^2$	$lb_f/100\ ft^2$	τ_y/YP
1	26-lb/bbl Bentonite Slurry	8.63	14	8.25	0.75	0.03
1	33-lb/bbl Bentonite Slurry	8.69	33	36	4.2	0.17
1	Ester-Based Fluid	8.27	36	63	22.9	0.36
1	Welan Gum Biopolymer Fluid	8.34	7	23	10.73	0.46
2	Lab Xanthan Gum Biopolymer Fluid	8.6	8	16	7.4	0.46
2	Field Xanthan Gum Biopolymer Fluid	9.8	12	23	6.3	0.27
3	Unhydrate Bentonite in Brine	8.8	2	1	0	0.00
3	Polymer-Coated Ultra-Fine Barite Fluid	13.5	18	15	4.7	0.31
3,5	Synthetic-Based Mud	14.2	49	16	4	0.25
4	Hollow Glass Sphere Fluid	8.4	11	33	8.9	0.27
6	Synthetic-Based Mud	11.55	34	24	7.03	0.29

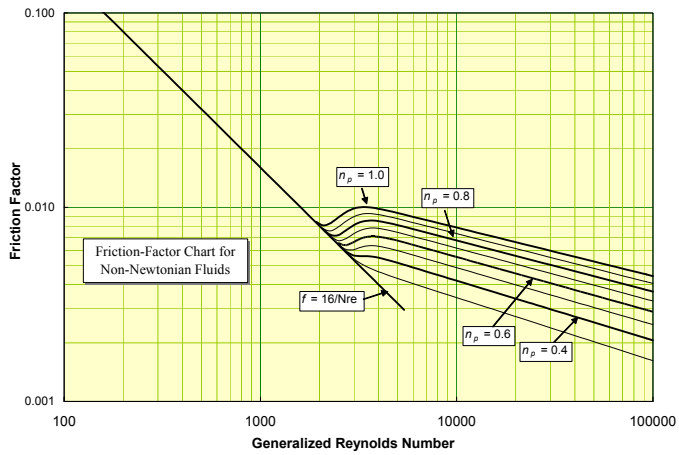

Fig. 1 – Fanning friction-factor chart for non-Newtonian fluids based on Eqs. 9-13.

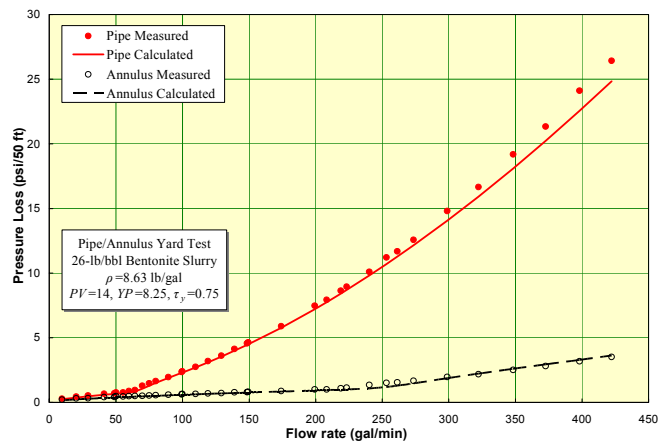

Fig. 2 – Demonstration of excellent agreement between measured and calculated pressures for a bentonite slurry tested in Test Facility 1.

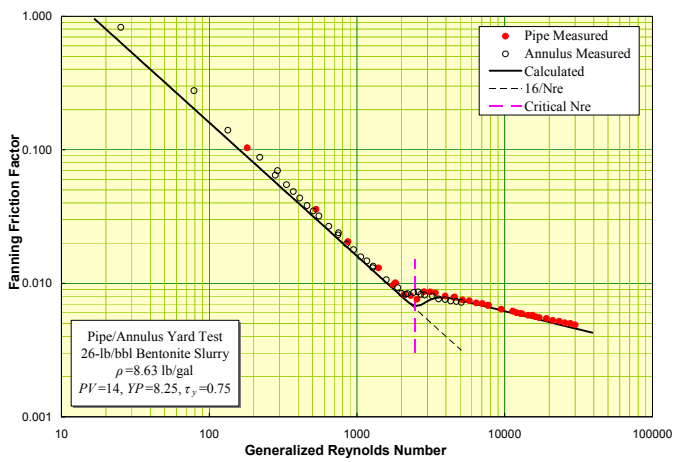

Fig. 3 – Friction-factor chart of data from Fig. 2 delineating transition zones.

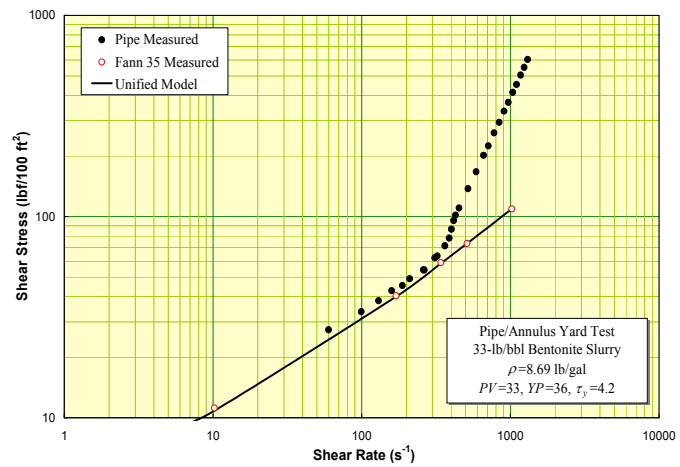

Fig. 4 – Rheogram demonstrating good agreement among pipe, viscometer, and model shear stresses.

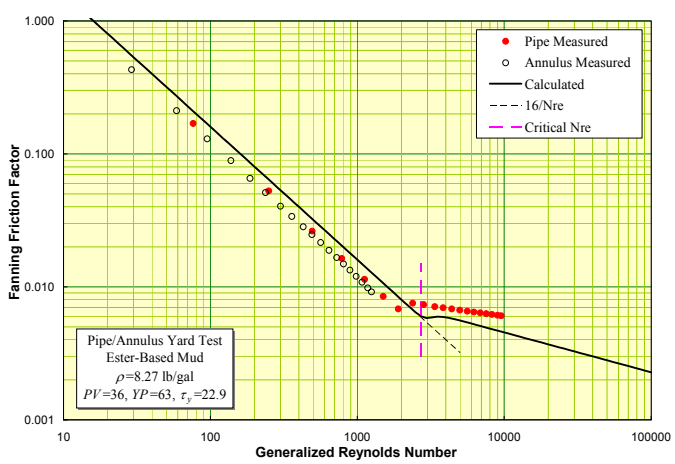

Fig. 5 – Friction-factor chart showing poor agreement probably caused by differences in flow-loop and viscometer test temperatures.

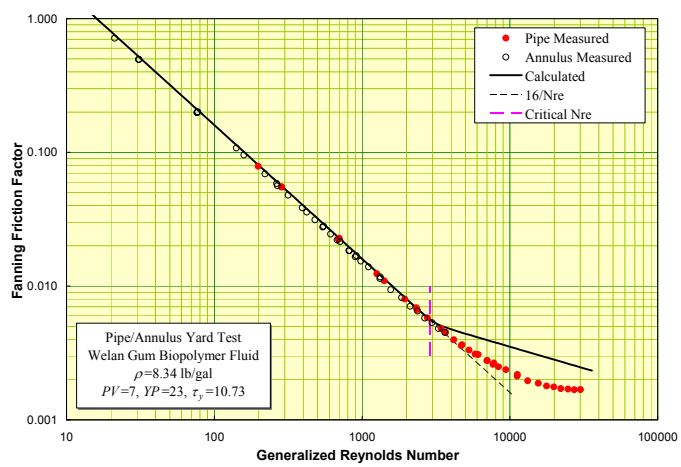

Fig. 6 – Illustration of drag reduction for a biopolymer fluid tested in Test Facility 1.

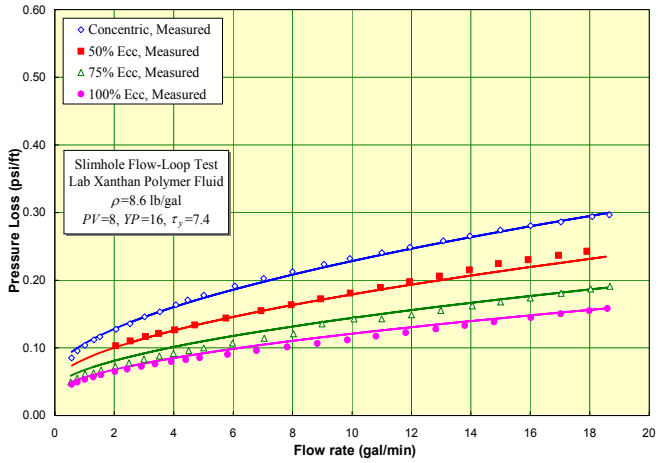

Fig. 7 – Eccentricity effects for a lab mud measured in Test Facility 2 showing excellent agreement among measured and predicted values.

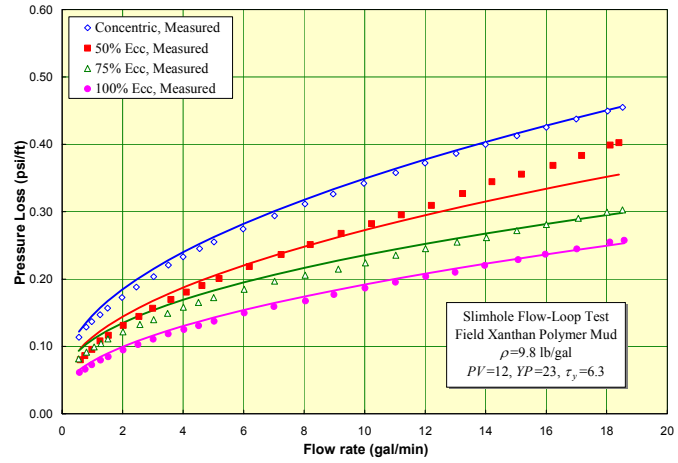

Fig. 8 - Eccentricity effects for a field mud measured in Test Facility 2 showing excellent agreement among measured and predicted values.

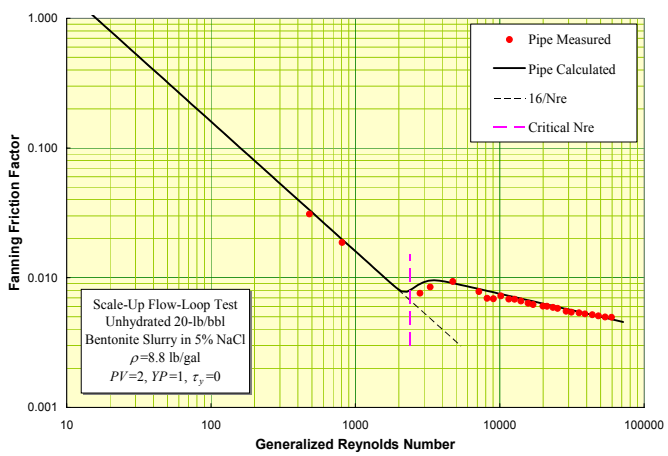

Fig. 9 – Friction-factor chart for an unhydrated gel slurry tested in a small-diameter, scale-up flow loop (Test Facility 3).

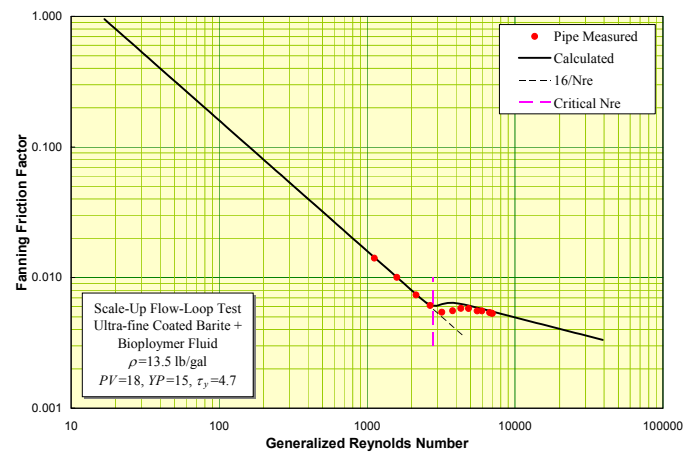

Fig. 10 - Friction-factor chart for an coated, ultra-fine barite slurry tested in a small-diameter, scale-up flow loop (Test Facility 3).

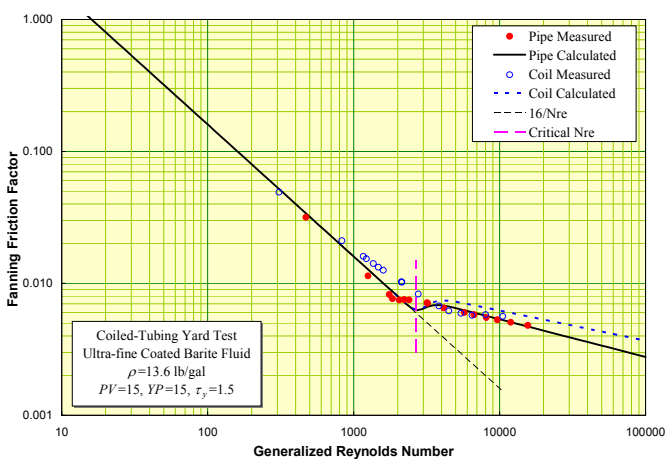

Fig. 11 – Friction-factor chart comparing measured and calculated results for straight pipe and reeled coiled tubing (Test Facility 4).

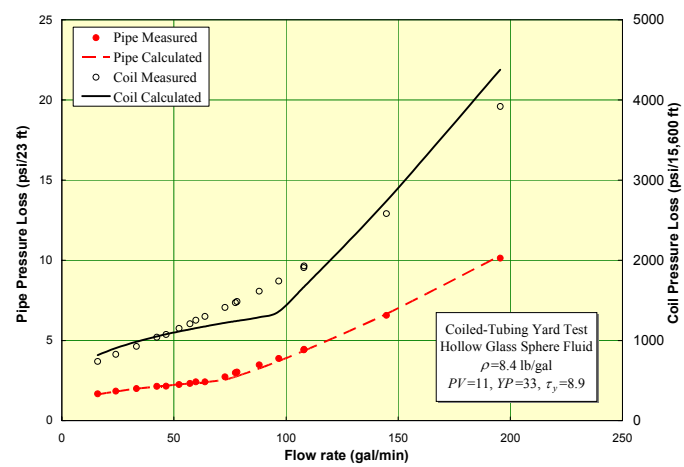

Fig. 12 – Pressure chart comparing measured and calculated results for straight pipe and reeled coiled tubing (Test Facility 4).

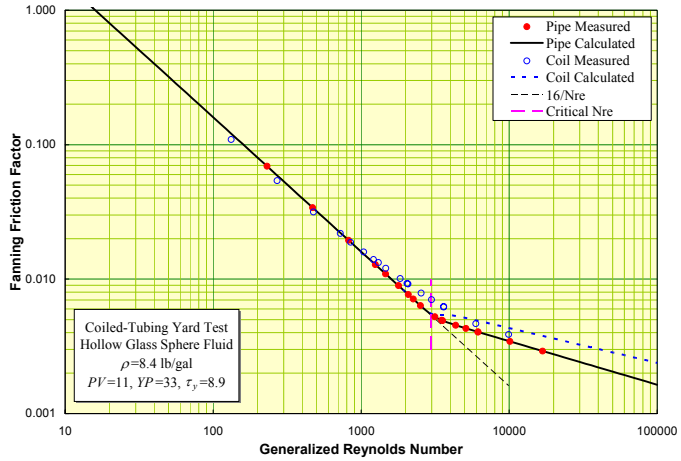

Fig. 13 – Friction-factor chart for the same data set used in Fig. 12.

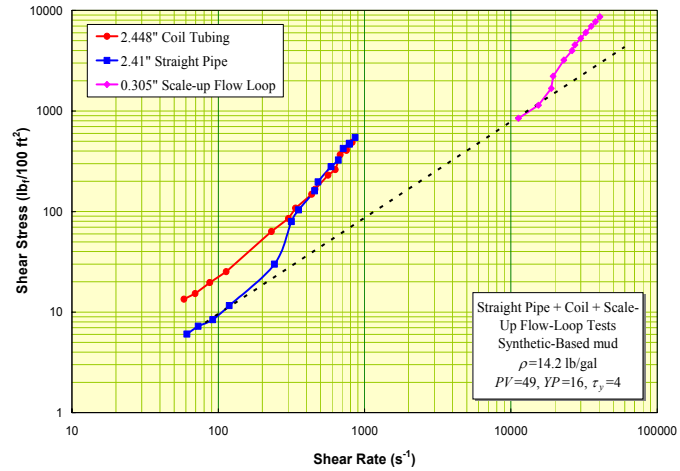

Fig. 14 – Rheogram for synthetic-based mud tested in three different geometries showing coiled-tubing and turbulent-flow diameter effect.

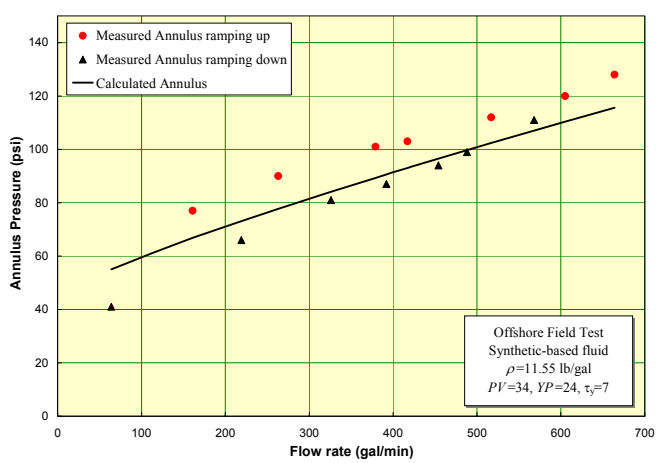

Fig. 15 – Comparison of measured and calculated annular pressure losses in an offshore well.[12]

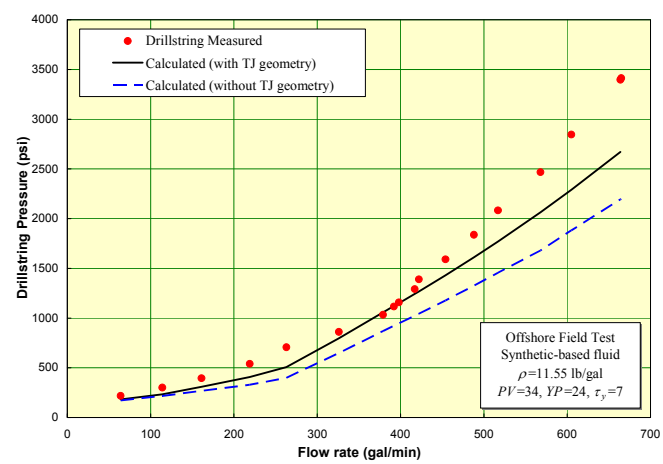

Fig. 16 - Comparison of measured and calculated drillstring pressure losses in an offshore well,[12] including contribution of tool-joint geometry.